Geologica Acta, Vol.12, Nº 4, ALAGO Special Publication. December 2014, 287-306
DOI: 10.1344/GeologicaActa2014.12.4.2

geologica acta

Subduction consequences along the Andean margin: thermal and topographic signature of an ancient ridge subduction in the Marañón Basin of Perú

R. BAUDINO[1] and W. HERMOZA[2]

[1]Repsol Exploration S.A.
Méndez Alvaro 44, 28045 Madrid, Spain. Email: robaudino@repsol.com

[2]Repsol USA
2455 Technology Forest Blvd, The Woodlands, TX 77381, USA. E-mail: whermoza@repsol.com

ABSTRACT

All along the eastern border of the Andes lie foreland basins that are among the most prolific hydrocarbon provinces of the world. Their Cenozoic evolution was controlled by the Andean uplift and its consequences on deformation and sedimentation. In turn, the Andean uplift results from the interplay between the subducting Nazca oceanic plate and the South American continental plate. Although the process exists all along the margin, the subducting plate is not regular including bathymetric anomalies and segments that result in different response in the deformation and active volcanism of the overriding plate. In the Marañón Basin of Peru, evidences allow documenting the consequences of a topographic anomaly subduction on the thermal regime and deformation of the Andean foreland during the Neogene. In this basin, a maturity anomaly is difficult to explain by considering only the present day thermal regime. However, it spatially coincides with the trace of a lost subducting ridge, the Inca Plateau. Other features like differential uplift and erosion can be related to the same event in the area. We review the consequences of oceanic ridge subduction along the Andean margin. Their effects on the deformation and volcanism of the forearc and arc regions have been extensively described. Their influence on the present day foreland topography is testified by the existence of giant alluvial fans and displaced terraces. Their effect on magmatism and ore deposits formation has also been demonstrated. The example illustrated here shows that their influence on thermal regime, deformation, erosion and ultimately on petroleum systems must also be taken into account in the search for hydrocarbons in subduction related basins.

KEYWORDS | **Andes. Marañón Basin. Neogene. Subduction. Oceanic ridge. Maturity anomaly.**

INTRODUCTION

For approximately the last 200Ma eastward subduction of the oceanic Nazca plate beneath the continental South American plate has been active. It is well known that an oceanic subducting plate is not regular but presents bathymetric anomalies and segments that result in different responses in the deformation and volcanism of the overriding plate. Among these anomalies are seamounts, seismic and aseismic ridges, hotspot chains and oceanic plateaus (*e.g.* Chung and Kanamori, 1978; Cloos, 1993).

Along the Andean margin several topographic anomalies have been observed on the surface of the subducting Nazca plate (Fig. 1A). Their continuity at depth is characterized by flat subduction angle (Gutscher *et al.*, 2000a) and coincide with a gap in the spatial distribution of active volcanism (Barazangi and Isacks, 1976) and with higher rates of uplift and erosion in the overriding plate (Ranero and von Huene, 2000; Clift *et al.*, 2003; Hampel *et al.*, 2004). Not only the present day spatial segmentation of the Andes can be documented, but also plate dynamics variation through time (tectonic events, changing subsidence and uplift rates, volcanic arc displacement) that have also been induced by oceanic ridge collisions (Ramos, 2005). In terms of mineral resources it was suggested that tectonic changes associated with impingement of aseismic ridges into the subduction zone may have triggered the formation of Andean ore deposits (Rosenbaum *et al.*, 2005).

Given the fact that so many processes are influenced it is reasonable to think that the whole dynamics of the system is affected by the subduction of topographic anomalies. It is therefore also reasonable thinking that the latter can also affect petroleum systems in associated Andean basins.

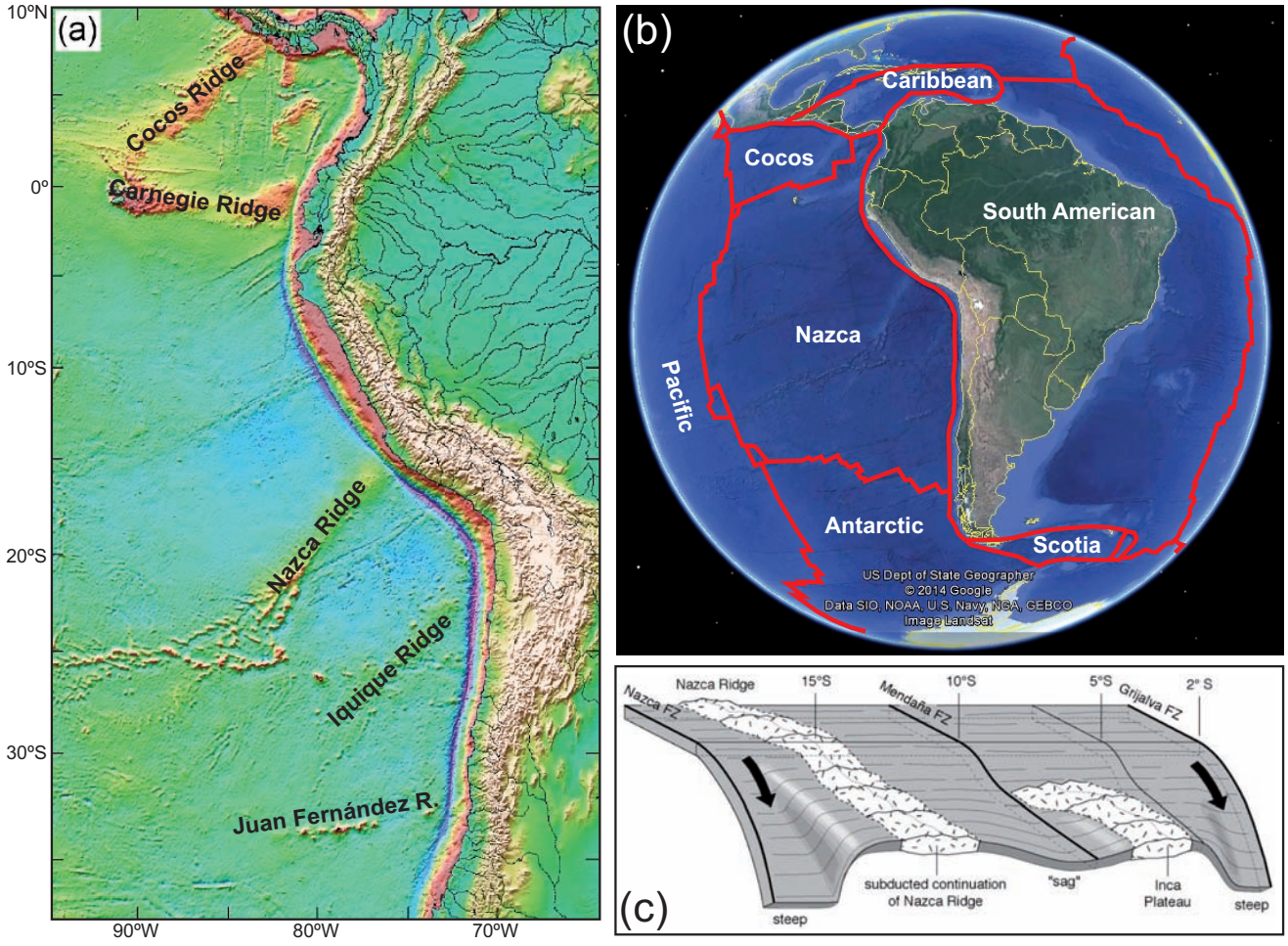

FIGURE 1. A) Topographic image of the eastern Pacific Ocean and the South American Andes highlighting the aseismic ridges subducting the South American continental plate (modified from Smith and Sandwell, 1997); B) 3D elevation map of the earth showing boundaries of the tectonic plates interacting with the South American plate (modified from USGS/Google); C) 3D perspective sketch of the Nazca Plate geometry and the flattening of its subduction angle consequence of two buoyant ridges each holding up a 500km section of the Plate with a sag in between (from Gutscher *et al.* 1999b).

Geologica Acta, 12(4), 287-306 (2014)
DOI: 10.1344/GeologicaActa2014.12.4.2

RIDGE SUBDUCTION ALONG THE ANDEAN MARGIN AND THEIR EFFECTS

All along the 7000km of the western margin of South America run the Andes, one of the longest continental mountain range in the world. The Andean margin is the reference example for oceanic-continental convergent margins: the orogeny, as well as modern seismicity and volcanism of the Andes are related to the subduction of an oceanic lithosphere, underlying the Pacific Ocean, beneath continental South America. This ongoing process has been active for approximately the last 200Ma and also controls the evolution of associated sedimentary basins such as the foreland ones extending east of the Andes. The structure of the Pacific oceanic lithosphere is complex and made of several tectonic plates. The Nazca plate is nowadays subducting beneath most of the Andean margin, from Colombia to Chile, and it is bounded to the north by the Cocos plate, subducting Central America, and to the south by the Antarctic plate, subducting southern Chile (Fig. 1B).

The surface of oceanic plates is not regular but presents bathymetric anomalies and segments. Among these anomalies are seamounts, seismic and aseismic ridges, hotspot chains and oceanic plateaus that result from mantle processes distinct from those forming oceanic crust at divergent plate boundaries. They are usually the result of volcanic activity bringing melted mantle rocks to the sea-floor. The continuous volcanic activity can led to the formation of isolated mountains with peaks below the ocean surface (seamounts) or elongated highs (ridges and plateaus) which can extend for hundreds and even thousands of kilometers. This pattern is caused by the sea floor plate moving over a stationary "hot spot" deep in the earth's mantle. The cessation of volcanism or a change in the orientation of the plate motion will cause the end of the building of a specific bathymetric anomaly and eventually the creation of a new ridge. When they are carried by subducting plates these volcanic constructions can end interacting with the overriding plate and eventually disappear underneath.

An important observation along the Andean margin is that areas involving the subduction of topographic anomalies are commonly characterized by a flat slab (Gutscher *et al.*, 2000a; Gutscher, 2002). In fact, flat subduction occurs at about 10% of the earth modern convergent margins, and most of these regions correlate with a subducting plateau or aseismic ridge (Mc Geary *et al.*, 1985; Gutscher *et al.*, 1999a,b; Gutscher *et al.*, 2000a). The influence of buoyant crustal blocks on the subduction geometry has been mentioned since the late seventies (Barazangi and Isacks, 1976; Pilger, 1981; Nur and Ben-Avraham, 1981; Sacks, 1983; Mc Geary *et al.*, 1985). Whereas a "normal" subducting oceanic plate sinks into the mantle at an angle close to 30° these areas tends to flatten (Fig. 1C). The explanation to flat subduction is the variation in lithospheric buoyancy related to an overthickened crustal block and its preservation at depth by a delay in the basalt (gabbro) to eclogite transition due to the cool thermal structure of two overlapping lithospheres (Gutscher *et al.*, 2000a). The thicker oceanic crust portion is underlain by a proportionally thicker harzburgite layer. During subduction, the gabbroic or basaltic crust transforms into eclogite. Eclogite and harzburgite have compositional buoyancies of opposite sign relative to undepleted mantle material (Irifune and Ringwood, 1993) that approximately cancel each other within an oceanic lithosphere. Once eclogitisation starts, the thickened subducting slab tends to lose its compositional buoyancy and will progressively recover a normal dipping angle. The conditions (temperature, pressure, hydration, stress) and depth at which eclogitisation occurs are still under debate.

Other mechanisms have been proposed to explain flat subduction: i) nonhydrostatic pressure forces (Jischke, 1975), ii) slab suction force (Stevenson and Turner, 1977; Tovish *et al.*, 1978), iii) rapid absolute motion of the overriding continent (Cross and Pilger, 1982; Vlaar, 1983), iv) subduction of very young, warm and thus buoyant lithosphere (Sacks, 1983; Cloos, 1993; Kirby *et al.*, 1996) and v) curvature of the margin (Bevis, 1986; Cahill and Isacks, 1992; Gephart, 1994). However, all these alternative explanations demonstrated to be weak (Gutscher, 2002) and the striking spatial relationship between flat slab areas and buoyant oceanic topographic anomalies suggest an important influence of the latter on the subduction process. Additionally, van Hunen *et al.* (2002) determined the viability of shallow flat slab development in the presence of a subducting 'buoyant plateau' with a two-dimensional finite element numerical model: with the only buoyancy mechanism a thickened portion of the oceanic lithosphere is enough to produce a flat-slab segment of 300km long.

In addition to produce a complex geometry of the subducting plate, flat subduction also might affect its stress field. A nearly 90° rotation of the stress field from the flat-slab region proper to the lateral contortion and a significant rotation downdip near the second inflection point have been found at the southern termination of the Peruvian flat-slab by studying focal mechanisms of intermediate depth earthquakes (Schneider and Sacks, 1987). Notice, however that this stress field rotation is challenged by Pardo *et al.* (2002) in the Central Chile subduction zone.

Topographic anomalies within the subducting Cocos and Nazca plates include from north to south (Fig. 1A) the Cocos Ridge (Ranero *et al.*, 2000), the Carnegie Ridge (Lonsdale, 1978), the Nazca Ridge (von Huene *et al.*, 1996; Hampel, 2002; Clift *et al.*, 2003; Hampel *et al.*,

2004), the Iquique Ridge (Gutscher *et al*., 1999a), and the Juan Fernandez Ridge (von Huene *et al*., 1997).

Not only are the geometry and stress field of the Nazca subducting plate affected by the presence of oceanic topographic anomalies. Response of the overriding continental plate in terms of thermal structure, seismicity and deformation style, uplift and erosion rates, distribution of volcanism and even ore deposits occurrence appear also to be affected.

Effect on thermal regime, seismicity and deformation style

Subduction margins are characterized by the existence of a wedge of hot convecting asthenosphere between the plunging oceanic plate and the overriding continental plate. Thus, the angle of subduction will define the extension of the wedge and greatly affect the thermal structure of the margin. This thermal effect was well illustrated by Henry and Pollack (1988) with heat flow measurements from Bolivia and Perú. They observed a high heat flow (50–120mW/m^2) in Bolivia above a normal (steep) subduction angle (300 to 500km from the trench), when low values (30–70mW/m^2) were measured above the Perú flat subduction. The difference can be explained by the presence of an underlying convecting asthenosphere and a local volcanic arc in the Bolivian normal subduction, whereas the wedge is absent or reduced and substituted by a cool oceanic slab (Nazca slab) in the Peruvian flat subduction.

Gutscher (2002) presented a statistical analysis of the upper plate seismicity along the Chilean margin from 20 to 40°S, covering the Andean orogenic area between the forearc and the stable South American craton. He demonstrated that the seismic energy released in the overriding plate above the central Chilean flat subduction segment is on average five times greater than in the Central Andean segment of Bolivia above normal subduction. The difference is nearly a factor of 10 between central and southern Chile. This phenomenon is also observed in the central Andes of Perú and in the northern Andes (Gutscher *et al*., 2000a) (Fig. 2). The observation of an increase in the seismicity above flat subduction segments implies a higher degree of interplate coupling, that is consistent with a greater contact area between the plates and a cooler thermal regime (stronger rheology) (Gutscher, 2002). Published focal mechanisms show predominantly compressional to transcurrent stresses with P-axes perpendicular to the trench suggesting an effective transmission of the subduction boundary stress to the overriding plate (Jordan *et al*., 1983; Suarez *et al*., 1983; Gutscher *et al*., 2000a). Thick-skinned deformation of the overriding plate is associated to flat subduction and increased coupling, resulting in large-scale block-type basement uplifts in the Pampean Range of Argentina (Jordan *et al*., 1983; Smalley *et al*., 1993; Ramos *et al*., 2002), the Eastern Cordillera of Colombia (Gutscher *et al*., 2000a) and in the Merida Andes of Venezuela (Ramos *et al*., 2004). Intraplate coupling also appears to be an important factor affecting strain partitioning in cases of oblique convergence like is the northwestern Andean margin of Ecuador where major strike-slip movement occurs along the Dolores-Guayaquil Megashear (Kellogg and Vega, 1995). There, dextral slip occurs 300–400km from the trench, at the level of the adakitic volcanic arc and appears to be caused by increased coupling above the Carnegie Ridge flat slab segment (Gutscher *et al*., 1999a). However, this portion of the South American plate is characterized by the presence of allochtonous accreted blocks separated by crustal sutures that also contribute greatly in the strain partitioning at least since the Late Paleogene (Baudino, 1995; Marocco *et al*., 1995).

Effect on uplift and erosion rates

Clift *et al*. (2003) demonstrated that the subsidence of the Lima Basin, in the Peruvian forearc, is controlled by tectonic erosion related to the obliquely subducting Nazca ridge. Seismic and well data (from the Ocean Drilling Program and Deep Sea Drilling Project - LEG 34) allowed them to reconstruct rates of erosion through time. Since 47Ma up to 148km of the plate margin have been eroded, and approximately 110km of that total appears to be lost since collision of the Nazca Ridge occurred, showing that the subduction of the ridge accelerates tectonic erosion in this portion of the forearc. Hampel *et al*. (2004), made a comparison with the Peruvian and northern Chilean forearc systems that are currently not affected by ridge subduction. They observed that the geological record significantly differs at 9°S, where the ridge did not affect the margin, from the Lima Basin area (11.5°S), where the ridge crest passed 9.5Ma ago (Hampel, 2002), and the present collision zone at 15°S. Whereas the margin at 9°S has subsided more than 1000m for 12–13Ma, the region at 11.5°S has undergone a phase of uplift and enhanced tectonic erosion during 11–7Ma with subsequent subsidence of more than several hundred meters since 6Ma (von Huene *et al*., 1988; von Huene and Lallemand, 1990; Clift *et al*., 2003). Based on these observations they proposed that the passage of the Nazca Ridge along the continental margin induces temporarily more intense tectonic erosion superimposed on a long-term erosive regime. Sandbox experiments by Dominguez *et al*. (2000) confirmed the erosion and deformation of the upper plate induced by seamount subduction. They observed a substantial shortening and thickening of the deformable seaward termination of the upper plate basement, associated with basal erosion. Seamount subduction induces significant material transfer within the accretionary wedge, favors large tectonic erosion

Geologica Acta, 12(4), 287-306 (2014)
DOI: 10.1344/GeologicaActa2014.12.4.2

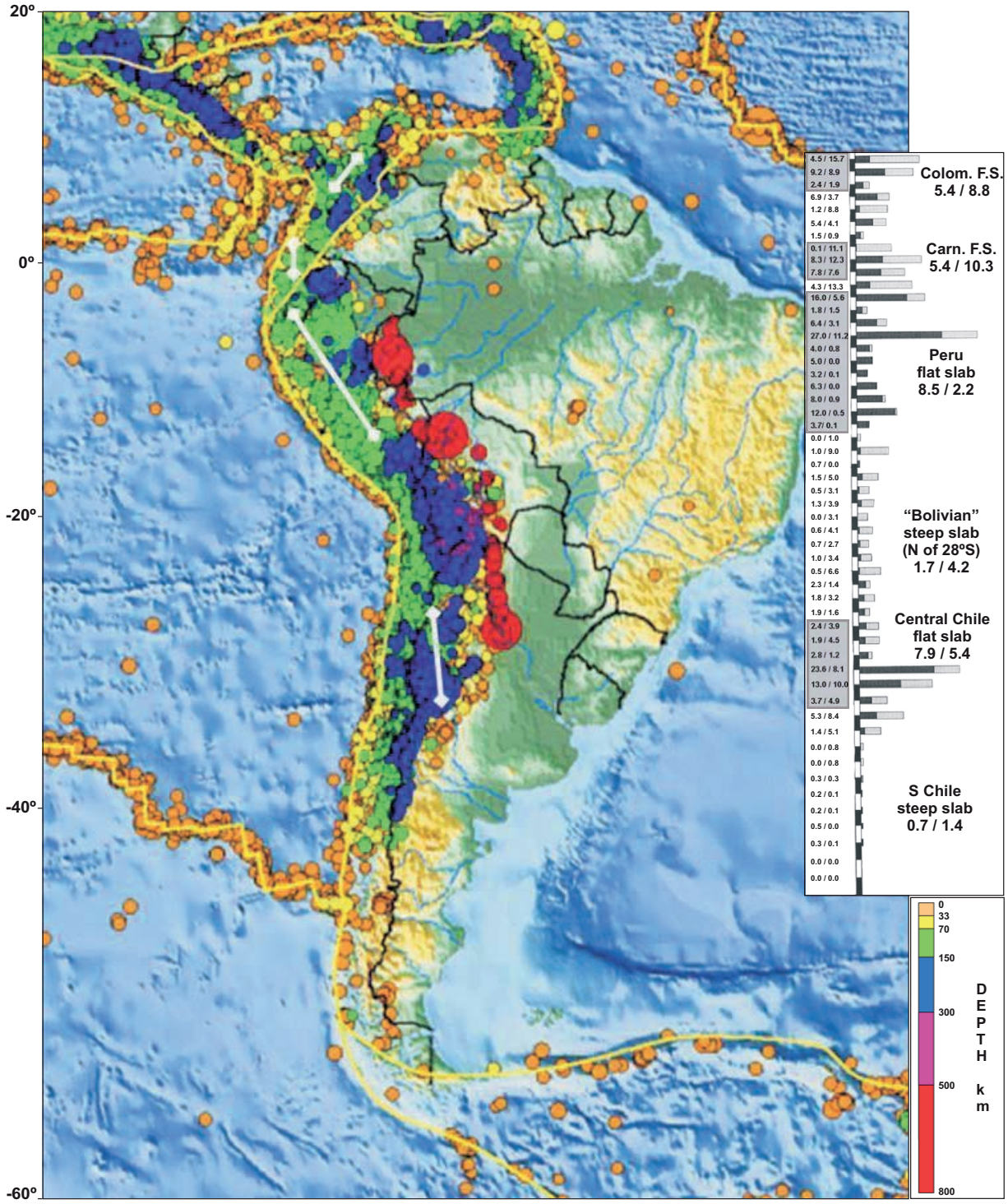

FIGURE 2. Seismicity and plate tectonic setting of South America. Seismicity is from a public USGS map showing 1990 to 2006 earthquakes hypocenters with a colour-coded depth (right scale). Notice how plate boundaries (yellow lines) are marked by shallow earthquakes while ridges are aseismic. Along the Andean margin the depth of the Benioff plane can be estimated from the depth of earthquakes and flat subduction zones (white thick brackets on map) are suggested (especially the Peruvian flat slab between 2 and 14°S). At the bottom right, histogram of seismic energy released in the upper plate 250-800km from the trench between 8°N to 44°S (energy in 10^6 J) from Gutscher *et al.* (2000a). N-S width of sampling box is 1°. Grey shaded boxes outline the flat slab segments, with pair of numbers indicating seismic energy released in the period 1900-1963 (left) and 1964-1995 (right). At the top right the major steep and flat Andean segments are indicated. Associated numbers indicate the averages of seismic energy released per 100km margin length for each segment.

of the frontal margin and thickening of the rear part of the margin. Numerical models by Groome and Thorkelson (2009) show significantly higher uplift rates in the forearc above the subducting ridge than along the periphery.

The previous examples refer to the forearc region of the subduction but evidences of ridge subduction effect on uplift and erosion in the intermontane and foreland domains are not so well documented.

We already mentioned the basement uplifts in the Pampean Range of Argentina and in the Northern Andes of Colombia and Venezuela associated to flat subduction. McNulty *et al.* (2003) indicated through paleomagnetic studies that Neogene counterclockwise rotations in the Eastern Cordillera of Perú were a result of the southward migration of the Nazca Ridge. The best documented example of foreland uplift related to ridge subduction in the Andes is probably the Fitzcarrald Arch of Perú. This major topographic feature (mean uplifted surface of ca. 600m a.s.l and area of ca. 4.105km^2) extends from southern Perú to western Brazil in Amazonia (Fig. 3). Espurt *et al.* (2007) documented its uplift since 4Ma (although it could have initiated slightly before this paroxysmal phase, N. Chigne pers. com.) and concluded that it was in response to the Nazca Ridge flat subduction that triggered vertical motion in the overriding South American plate as far as 750km inboard of the trench. A similar process could be active in Ecuador since Pleistocene, where Bés de Berc *et al.* (2004) related the morphology changes and tectonic uplift of the foreland in the area of the Pastaza alluvial mega-fan to the subduction of the Carnegie ridge (Fig. 3).

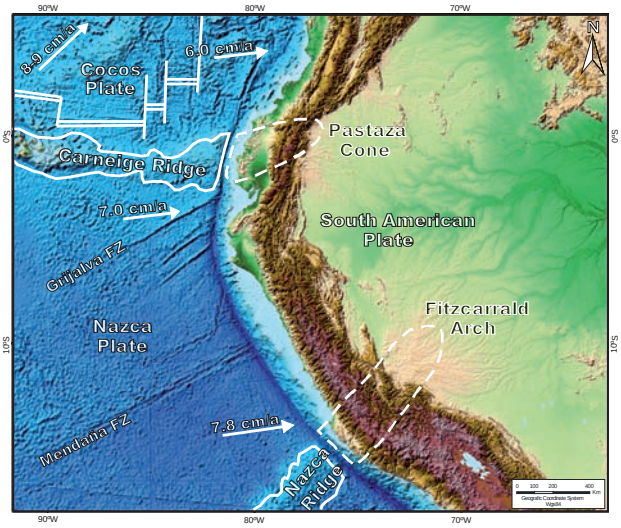

FIGURE 3. Tectonic setting of the northern and central Andean margin with topographic map of the South American plate (elevation map from NASA/Jet Propulsion Laboratory) showing the coincidence between the Carnegie and Nazca ridges, with their inferred extension at depth (dashed outline), and the Fitzcarrald Arch and Pastaza Cone foreland uplifts. Contour of ridges with their extension at depth are from Gutscher *et al.* (1999a, 2000a). Plate convergence vectors are from Gutscher *et al.* (2000a).

Effect on volcanism

The relationship between ridge subduction and overriding plate volcanism has been discussed by several authors (Nur and Ben Avraham, 1981; Jordan *et al.*, 1983a, 1983b, McGeary *et al.*, 1985) noting that their continuity at depth coincides with a limit in the spatial distribution of active volcanism.

Ramos (1999) divided the present Andean arc in four zones of active volcanism (Fig. 4): the northern Volcanic Zone (5°N to 2°S), in southern Colombia and northern Ecuador, the central Volcanic Zone (16°S to 26°S) between southern Perú and northern Chile, the Southern Volcanic Zone (34°S to 46°30'S), in central Chile and Argentina, and the Austral Volcanic zone, south of 47°S. The nature and composition of volcanism in each zone is specific, depending on the continental crust thickness and composition (presence of accreted allochtonous terranes can introduce variations), presence of deep crustal faults (limiting allochtonous terranes for example), angle and age of the subducting plate, presence and geometry of an asthenospheric wedge, geometry at the transition between slabs with different subducting angles (continuous or through a tear zone).

The Andean active zones are separated by volcanic gaps that are visibly associated with flat subduction (Fig. 4): in Colombia and Venezuela, north of 5°N; in Perú between the Gulf of Guayaquil (2°S) and Arequipa (14°S); in Chile-Argentina, west of the Sierras Pampeanas (27 to 33°S) and south of the Chile Rise-Trench triple junction between the South American, Nazca and Antarctic Plates (46 to 49°S).

The genetic relationship between subduction of aseismic ridges and flat-slab occurrence appear then to be the main cause of volcanic activity conclusion in Perú and Northern Chile and Argentina. The collision of seismic ridges also produces a volcanic arc gap, but with an unusual suite of near trench magmatism, plateau basalts, and adakites as observed in the Patagonian volcanic gap (refs. in Stern, 2004).

Regarding a possible mechanism, Isacks and Barazangi (1977) mentioned the remarkable coincidence between the nearly flat Benioff zones of Perú and central Chile and the absence of Quaternary volcanoes, suggesting that andean volcanism requires a wedge of asthenosphere between the subducted and upper plates. Thorpe (1984) concluded that Andean magmatism was initiated by the dehydration of the subducted oceanic lithosphere. Dehydration reactions cause

Geologica Acta, 12(4), 287-306 (2014)
DOI: 10.1344/GeologicaActa2014.12.4.2

FIGURE 4. Topographic map of South America where the shape of the subducted oceanic plates at depth has been superimposed. The spatial relationship between absence of volcanism and flat subduction is shown (contours from Ramos, 1999; elevation map from NASA/Jet Propulsion Laboratory. Triangles are active volcanoes).

blueschist and eclogite facies to form at depth in the vicinity of the subducted slab. Water released from these reactions invades the overlying mantle wedge lowering the temperatures required for its partial melting, which produces mafic magma, and in the crust produces felsic magma (Dickinson and Snyder 1979; Pilger 1981; Bird 1988; Ramos *et al.* 2002; English *et al.* 2003; Murphy, 2007). Large-scale slab melting is predicted only for the slowest and youngest subduction zones (van Keken *et al.*, 2002), and hence is very rare in the Andes. In this sense, the initial stages of generation of Andean magmas are similar to magma generation processes in oceanic convergent plate boundary island arcs, but are locally complemented by the participation of continental crust and/or subcontinental mantle lithosphere (as shown by isotopic composition of the northern SVZ and CVZ Andean magmas) (Stern *et al.*, 2004).

Dehydration of the slab is widely admitted to trigger Andean volcanism. The resulting fluxing of released fluids lowers the mantle solidus and initiates a chain of events culminating in the generation of magma that rises to form volcanic arcs. In addition, the descent of the subducting plate stirs up the mantle, bringing upward a current of warmer mantle material from greater depth (Tamura *et al.*, 2002). The location of slab dehydration reactions depends strongly on the temperature and pressure conditions at the top of the subducting plate and hence on the detailed thermal structure of subduction zones (van Keken *et al.*, 2002). Consequently, a clear mechanism explaining the absence of volcanism in flat subduction segments is hard to define as many varying parameters are intervening. However, the absence of an asthenospheric wedge appears to be the major cause, as it first results in the absence of mantellic material to interact with fluids produced by dehydration of the slab, and second the temperature affecting the upper part of the slab that is coupled to the overlying continental crust is relatively low and dehydration is reduced. Where active volcanism occurs, lateral extension and eventually displacement of the arc are controlled by the lateral extent of the slab dehydration zone and consequently by the subduction angle and velocity.

Not only the present day spatial segmentation of volcanism can be documented, but also the shifting and expansion, of the arc through time (Kay *et al.*, 1991; Ramos *et al.*, 1991; Kay and Abbruzzi, 1996). In the Sierras Pampeanas region of Argentina, Ramos *et al.* (2002) documented the eastward migration of arc volcanism between 16 and 15.8Ma and between 9.5 and 6.4Ma (2m.yr later than the 11Ma collision of the Juan Fernandez Ridge at this latitude) and related it to changes in the subduction angle. The last subduction-related volcanism occurred more than 750km east of the trench ending at approximately 8.6Ma in the Principal Cordillera and 1.9Ma eastward in the Sierras Pampeanas. In addition, these authors postulated another indirect consequence of flat subduction on volcanism: uplift and deformation followed the eastward migration of the volcanic arc and hence were likely related to thermal crustal weakening and the development of brittle-ductile transitions that in turn allowed the uplift of basement-cored blocks.

The Andes of the Neuquén region of Argentina (36,8–38,8ºS latitude) have distinctive characteristics that result from the alternation of periods of generalized extension followed by periods of compression. Different stages from Jurassic to Present are correlated with changes in the geometry of the Benioff zone through time by Ramos and Folguera (2009). Periods of subduction zone steepening are associated with large volumes of poorly evolved magmas (generated by injection and melting of hot asthenospheric material from the subcontinental mantle into the wedge) and generalized extension, while shallowing of the subduction zone is linked to foreland migration of more evolved magmas associated with contraction and uplift in the Principal Cordillera.

Effect on ore deposits formation

Rosenbaum *et al.* (2005) suggested that tectonic changes associated with impingement of aseismic ridges into the subduction zone may have been responsible for the formation of ore deposits in metallogenically fertile environments. Their study shows a spatial and temporal link between the subduction of the Inca Plateau, Nazca and Juan de Fernandez ridges and ore body formation in the Peruvian Andes during the Miocene. The authors stressed however that ridge subduction is not a necessary factor but may trigger favored geodynamic conditions. Fertile calc-alkaline magmas are generated in the MASH zone (zone of Melting, Assimilation, Storage and Homogenization), a relatively narrow band in the lowermost crust or mantle-crust transition, where mixing between mantle-derived melts and assimilated crustal rocks takes place during periods of stable subduction (Hildreth and Moorbath, 1988). This process may increase the metallogenic fertility, but ore minerals will eventually be deposited in response to cooling of the wall-rocks, fluid phase separation or mixing with external fluids allowing exsolution of the metalliferous and sulphur-rich hydrothermal fluids (Richards, 2003). Rosenbaum *et al.* (2005) postulated two possible mechanisms: i) Admitting that a large number of ore deposits in northern Perú developed immediately upon impingement of the edge of an aseismic ridge into the subduction zone, the authors assume that an important factor for their formation is the resulting change in the state of stress in the crust. Increased coupling between the two plates would lead to enhanced deformation and related faults could then mobilize fertile magmas in the MASH zone to travel towards shallower depths and finalize with exsolution of fluids. As stated by Cox *et al.* (2001), crustal deformation is also likely to

Geologica Acta, 12(4), 287-306 (2014)
DOI: 10.1344/GeologicaActa2014.12.4.2

increase permeability and to facilitate fluid pathways at shallow crust and melt pathways from depth; ii) we already mentioned that subduction of an aseismic ridge will result in slab flattening. When flat subduction occurs volcanism is likely to terminate or to be shifted to a different locus. The cessation of activity may prevent potential metal loss during eruptions and help their preservation in the magmatic reservoir, promoting rock/magma interactions and the formation of ore deposits. Another consequence of slab flattening is that the associated tectonic change is likely to lead to the termination of a magmatic cycle, thus promoting the occurrence of ore minerals in porphyry-type rocks. And finally, Rosenbaum *et al*. (2005) also envisaged that metalliferous fluids could be derived from melting of the subducting slab. These authors, however, mentioned that according to their results the development of flat subduction was not the primary mechanism responsible for ore deposits formation.

OVERVIEW OF THE MARAÑÓN BASIN PETROLEUM GEOLOGY

The Marañón Basin is located in the north-eastern part of Perú. Prolific in hydrocarbons, it is part of a larger foreland unit including the Oriente and Putumayo basins of Ecuador and Colombia (Fig. 5). This basin developed since the Jurassic times east of the rising Andean Mountains. Its actual foreland evolution is mainly the consequence of the subsidence of the South American plate, caused by flexuration resulting from the tectonic loading of its Pacific margin, and enhanced by sediment accumulation.

The sedimentary infilling of the Marañón Basin can be divided in three megasequences overlying the Paleozoic economic basement and corresponding to different tectono-stratigraphic settings (Fig. 5): i) a Pre-Cretaceous sequence that corresponds to a rift type evolution phase of the basin and starts with the Pucará Group. This Late Triassic–Jurassic carbonated sequence is penetrated by a limited number of wells in its uppermost layers, but seismic interpretation suggests that it was deposited in a N–S to NW–SE active rift system. However, outcrops have been described to the west of the basin and can be used to define a litho-stratigraphic framework (Fernández *et al*., 2002; Rosas *et al*., 2007). Of particular interest is the organic-rich Aramachay Formation that apparently sourced several hydrocarbon accumulations in the basin (Waples, 2002). The siliciclastic Saraquillo Formation of Jurassic to earliest Cretaceous age conformably overlies the Pucará Group. ii) The base Cretaceous unconformity is a regional feature also described in the Oriente and Putumayo basins that marks the transition to a wedging sequence of Cretaceous age. This megasequence contains most of the petroleum reserves of the Marañón Basin into high porosity and large extension marine to littoral sandstones like the Vivian, Chonta and Agua Caliente Formations Source rocks like the Raya and Chonta Formations were deposited during transgressive events. iii) Finally during the Late Cretaceous–Tertiary times the Marañón Basin entered into a classic foreland type evolution responding to the increasing uplift of the Andes, the westernmost part of the former basin being cannibalized by the eastward motion of the fold and thrust belt. Inside this megasequence a potential source rock with associated reservoir could exist in the Eocene Pozo Formation in basin foredeep locations.

The Marañón Basin has been producing oil since the 40's from the Cretaceous reservoirs, and Jurassic carbonates and Eocene sansdstones are considered potential reservoirs. Today it is still a place of active exploration.

BASIN MODELLING AND GEODYNAMIC IMPLICATIONS

In order to evaluate the petroleum potential of the Marañón Basin a 3D basin model was simulated. Although this is not the main purpose of this discussion and no maturity or migration result will be presented, it is important to understand how the basin modelling exercise led us to envisage large scale geodynamic processes.

Model construction

The construction of a 3D basin model is primarily based on 2 sets of input data. First, what are named structural data include map data such as depth structural maps, facies/lithology maps (with related petrophysical parameters) and eventually eroded thickness maps. Second, what we define as "geochemical" data include the map data that define each source interval characteristics (total organic carbon content (TOC), IH, kerogen type, etc.) and the generation kinetic schemes assign to each one. Once skeleton of the model is built we need thermal history scenarii before running simulations. This can be done through the construction of a set of basal temperature or heat flow maps (entering the basin at the base of the sedimentary filling) at different ages of the basin evolution, or in the more advanced softwares by setting crustal parameters (geometry, lithology, radiogenic heat production) with eventually stretching parameters in the case of rift basins (duration, stretching factors, multiple rifting events).

During this study ten key horizons were interpreted regionally along 2D time seismic lines, depth converted and mapped to generate a set of 2x2km grids covering the entire Marañón Basin (Fig. 6). Thirteen additional horizons were built from well markers interpolated through isopach mapping. Source and reservoir layers were individualized to finally define a set of 30 horizons with their corresponding stratigraphic age.

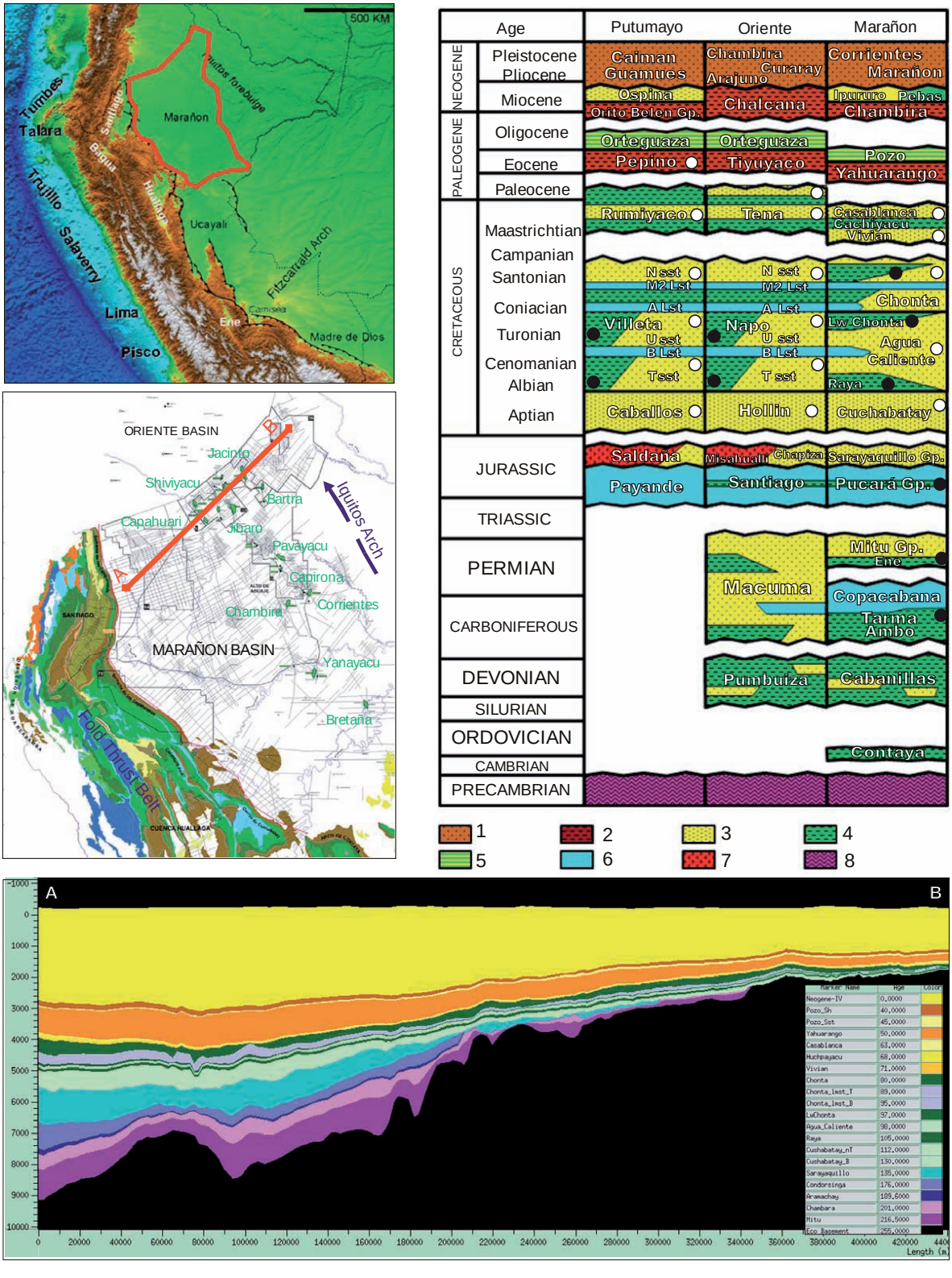

FIGURE 5. A) Location map of the Marañón basin and synthetic lithostratigraphic columns of the Putumayo, Oriente and Marañón foreland basins. Upper left: Marañón basin extension in Perú is outlined in red, names refer to sedimentary basins and structural elements; Center left: geological map with main oil producing fields, seismic coverage and trace of the geologic section shown below; Right: synthetic lithostratigraphic columns of the Putumayo (Colombia), Oriente (Ecuador) and Marañón basins mentioning main formations and lithologies. White dots indicate main producing reservoirs; black dots indicate main source rocks. Legend: 1- Molasse, 2-Red Beds continental deposits, 3-marine sandstones, 4-marine shale/marl, 5-fluvial to shallow marine sandstones and shales, 6-carbonates, 7-volcanics, 8-metamorphics.

Geologica Acta, 12(4), 287-306 (2014)
DOI: 10.1344/GeologicaActa2014.12.4.2

Two erosional unconformities were considered in the model: i) the base Cretaceous unconformity (BCU), that is regionally known and reflects a major change in the basin evolution from a rifting to a retroarc subsidence style. Its age was arbitrarily set in the model to 130Ma (estimated age of the first sediments of the Cushabatay Formation). Erosion started sometime between 135 (age of the youngest underlying deposits) and the 130Ma, and eroded thickness of the Pre-Cretaceous sequence was estimated between 0 and 2000m. The eroded thickness was initially set using bibliographic information and then adjusted during thermal calibration to fit maturity measurements (details in further sections); ii) the Inca Plateau unconformity has been identified during this study and it is of Pliocene age (arbitrarily set to 3.5Ma). Erosion existed only in the south-western part of the study area and its magnitude was defined during thermal calibration (see details in the corresponding section).

Basin models rely on petrophysical parameters (compaction curves, thermal conductivity, permeability, etc.) to perform first structural reconstruction (backstripping), and then thermal regime, maturation and migration calculation through time. These petrophysical parameters are lithology specific and that is why facies interpretation, either uniform or laterally variable, of each layer has to be converted into lithology maps. For the Cretaceous and Tertiary sequences, reservoir lithology mapping was based on sand/shale ratio when wells data were available (between 20 and 50 well over the basin depending on the stratigraphic interval, Fig. 6). If not, it was based on published depositional environment maps. Lithology maps of the non-reservoir layers of the Cretaceous and Tertiary sequences were defined using well data and published information. The Pre-Cretaceous sequence of the Marañón Basin was drilled partly by a limited number of wells and its stratigraphy is not well known (only log data from 3 wells located in the south-east could be used in this study). Facies and corresponding lithology maps were defined upon a new stratigraphic model defined by the authors and based on published data (Fernández *et al.*, 2002; Rosas *et al.*, 2007) and proprietary outcrops observation in the south-western bounding ranges extrapolated to the basin subsurface through seismic data.

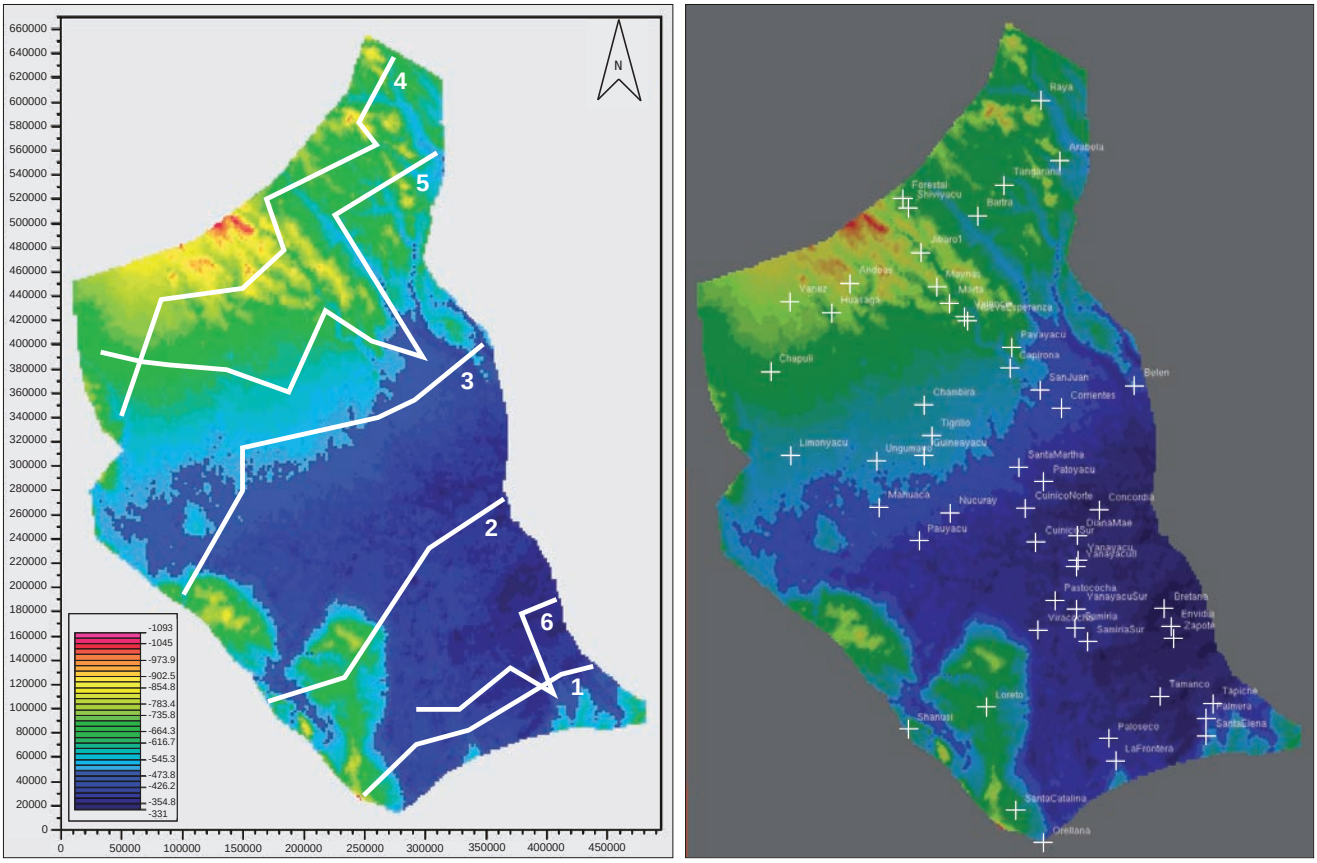

FIGURE 6. Topographic map of the Marañon basin showing the extension of the 3D basin model (UTM projection, distance in m). Elevation is in feet and negative values are above msl. Left: traces of 2D section extracted and used for initial calibration; Right: location of wells with data used for model calibration.

Several source rock layers are known in the Marañón Basin and oil-source correlations have been done showing that organic rich layers from both the Pre-Cretaceous and Cretaceous–Tertiary sequences have been contributing to the petroleum system (Wapples, 2002; Repsol Proprietary Information, 2008). For each source layer we defined a set of maps including lithology, organic facies or kerogen type, TOC content. A generation kinetic scheme was associated to each kerogen type.

Calibration Data

Measured data used to calibrate numerical models include mainly petrophysical data (porosity, permeability, etc.), temperature data (borehole and reservoir test temperature, surface heat flow, etc.) and maturity data (vitrinite reflectance, thermal alteration index, T_{max}, apatite fission track analysis, fluid inclusions analysis, etc.). Regarding the rock petrophysical properties, including thermal, we used as starting point the modelling software (Temis®) default parameters (compaction curves, permeability exponents, conductivity, etc.) and tuned them when necessary to obtain a satisfying calibration all over the study area. Porosity calculated by the simulator was checked against porosity values calculated from well logs or measured on cores at well location (Fig. 6).

The main objective of basin modelling is to simulate the maturation of source rocks and the subsequent generation of hydrocarbons. The main factor controlling maturation is the heat affecting the organic matter contained in source rocks and thus a robust thermal model through time must be constructed. The usual way of working is to start with an initial thermal model, compare the model calculation at well locations with measured data and refine it until reaching a satisfying calibration with various thermal histories or a single one in the best case. In such a foreland context, eroded thicknesses must eventually be also taken into account. An extensive database of thermal calibration data has been built using information from Repsol corporate database and public information (Fig. 6).

In order to optimize the time of calculation, thermal calibration was performed initially using fluid flow simulations along six 2D sections (Fig. 6). Thermal calibration of the model at well locations was checked again in 3D simulations.

Thermal history

Thermal data input for a basin model include: i) the rocks and formation water thermal properties that has been mentioned previously; ii) thermal upper boundary limit that corresponds to the surface temperature through time; this can be obtained from present day meteorological measurements and has to be reconstructed by user at different ages through time (in the same way are built paleotopography maps); iii) lower thermal boundary limit that corresponds to the basal heat entering the basin and can be set as heat flow (set by user or calculated by the program in function of the lithospheric properties) or using geothermal gradients; this is the most important parameter in terms of thermics and it must be based on a reliable geodynamic model for the basin; iv) in a complex structural setting like the Marañón Basin of Perú erosional events and eventually thermal anomalies associated to the Pacific plate subduction (volcanism, asthenospheric wedge retreat or expansion, thrust related crustal thickening, etc.) must also be considered.

First, a present day thermal regime must be defined by setting an upper boundary (the annual average surface temperature map) and a lower boundary map to calibrate the model with corrected well temperature data. When plotting temperature versus depth below mud line, a great dispersion is visible in the Marañón Basin with values that can vary up to 30ºC at the same depth (Fig. 7A). The basal heat flow (HF) values, required to calibrate temperatures measured in a well, were plotted on a map, showing a general increasing trend from west to east (Fig. 7B). This can probably be related to a thickest sedimentary cover in the western part of the basin as suggested by the isopach map of the infilling (Fig. 7C). As a consequence, a single value for the present day basal HF could not be considered and a spatially varying map was built, tying to the HF values required to calibrate at well locations and conditioned by the infilling thickness trend (Fig. 7B).

In a second stage, we established the historical thermal regime that has affected the study area through geological times. The only way to calibrate the basal heat flow at different ages, after creating reliable paleosurface temperature maps, is to use maturity measurements and, in the specific case of this study, vitrinite reflectance (Ro). When applying the present day basal HF through time a satisfying calibration of the calculated maturity is obtained only at the wells located in the north. In the south, Ro measured data are greater than the calculated ones indicating that the basal HF was greater in the past than today. In addition, where Ro measurements exist in the Pre-Cretaceous sequence they indicate an even higher maturity that cannot be explained only by the erosion at the BCU. Consequently, a thermal event generating a much higher HF has to be speculated before the Cretaceous. A continental rift evolution is known to have occurred in the basin during Jurassic time and the thermal event

Geologica Acta, 12(4), 287-306 (2014)
DOI: 10.1344/GeologicaActa2014.12.4.2

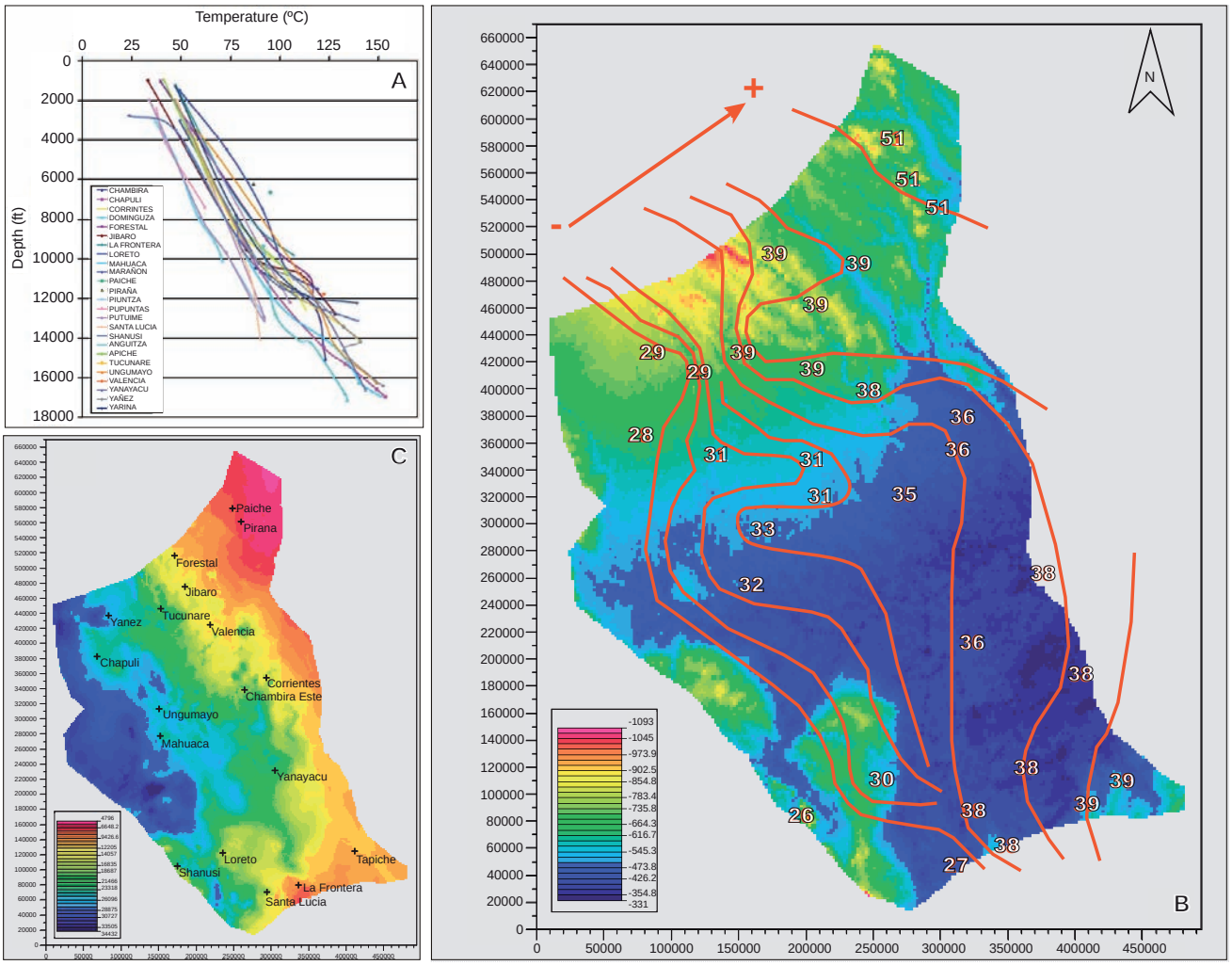

FIGURE 7. A) Burial depth vs. corrected borehole temperature graph showing great dispersion of Present day temperatures; B) basal heat flow values required to calibrate measured temperatures and related contours (values are in mW/m^2). Observe the general increasing trend from west to east; C) Isopach map of the Marañon basin total sedimentary infilling.

documented here can be related to it. As a result, a first modification of the thermal model consisted in introducing a higher basal HF during Pre-Cretaceous times (maximum value at the end of tectonic rifting and progressive decrease until present day values).

The discrepancy in maturity calibration of the model between the north and the south of the Marañón Basin in the Post-Jurassic sequence is more difficult to explain. The limited extension of the anomaly implies a local phenomenon but even harder to understand is which kind of control could lead to a recent and localized decrease in basal HF (Baudino and Hermoza, 2011). One could first think about a volcanic event but none is identified in the area. Another geodynamic cause must be invoked.

EVIDENCES OF AN ANCIENT RIDGE SUBDUCTION

When looking at the structure of the basin and especially its recent evolution an erosive event is visible in the south-western part as documented by seismic interpretation (Fig. 8). Indeed, the wedging of the Tertiary foreland deposits is disturbed here by a recent uplift that led to significant erosion of the Tertiary sediments. The location of the uplifted area can be appreciated when looking at the isopach map of the Neogene sequence (Fig. 8). A rough estimation of the missing section in 800 to 1200m can be made from the seismic information (Fig. 8). We tested the impact of this local erosion over maturity from wells of the area but it was not enough by itself to explain the discrepancy between calculated and measured maturity. Then the following question arises: what kind of regional

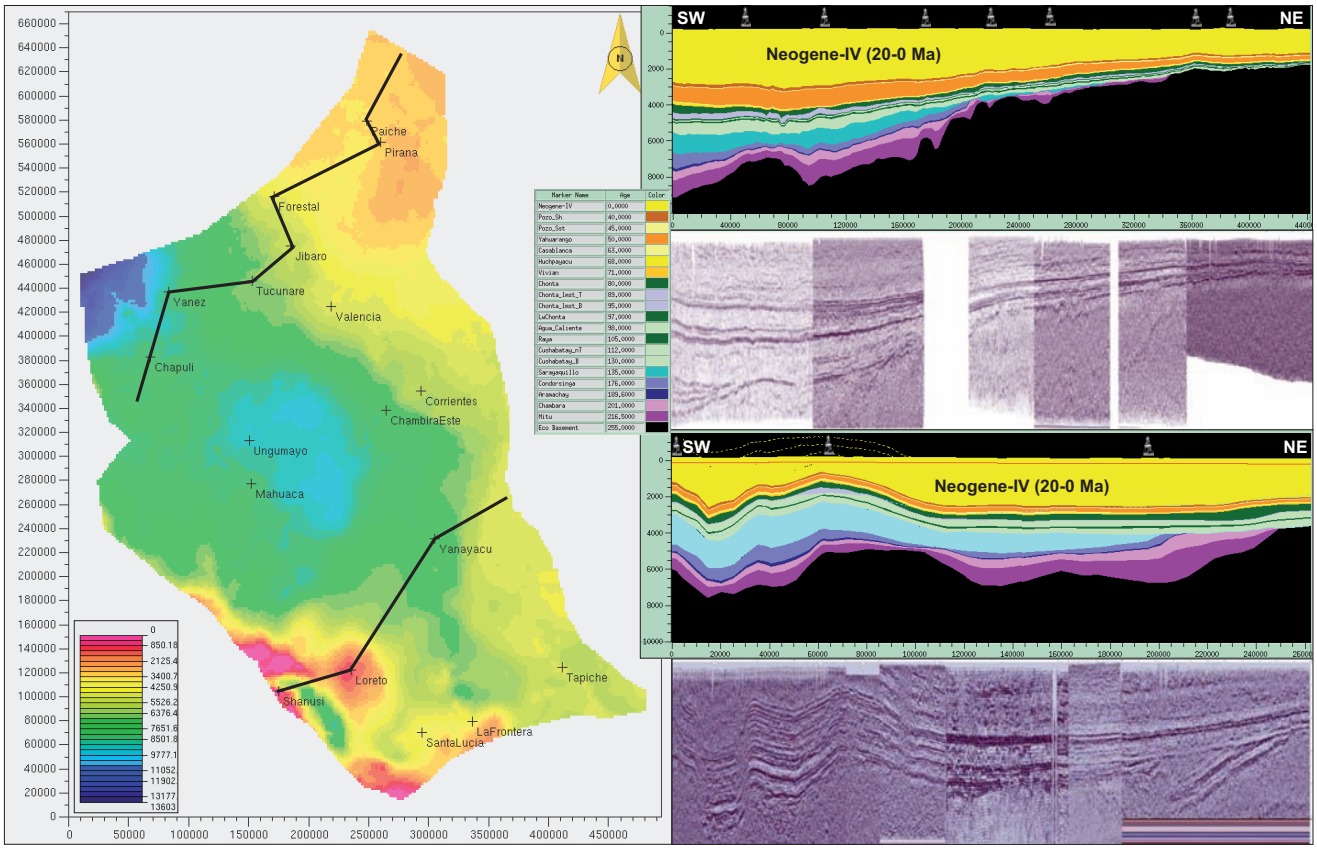

FIGURE 8. Isopach map (in feet) of the Neogene-IV sequence (ca. 20Ma to Present) with traces of the two stratigraphic section (scale in meters). Related 2D seismic sections are displayed on the right. Notice the recent uplift and erosion affecting only the south-western area of the Marañón basin. The missing section can be roughly estimated in 800 to 1200m in the southern seismic line.

event could have recently both decreased the basal HF and generated uplift in the south-western part of the basin at the same time?

Gutscher *et al.* (1999b) identified and documented the existence of a lost oceanic plateau they named the Inca Plateau, that subducted the South American plate during the Neogene (Fig. 9). The combined buoyancy of the Inca Plateau and Nazca Ridge would support the 1500 km long Peruvian flat slab of the South American Pacific margin. Their conclusions are the result of an analysis of the subducting Nazca plate seismicity, the structure and geochemistry of the Marquesas Plateau as well as tectonic reconstructions of the Pacific-Farallon spreading center between 34 and 43Ma. They stated that these data restore three sub-parallel Pacific oceanic plateaus that are the Austral, Tuamotu and Marquesas, to two Farallon plate (parent of the present Nazca plate) counterparts that are the Iquique and Nazca Ridges. The Inca Plateau would be the sixth and missing piece of an ensemble of hotspot tracks formed at on-axis positions (Fig. 9).

Rosenbaum *et al.* (2005) proposed a plate tectonic reconstruction showing the stages of the subduction at the Peruvian margin (Fig. 9).This takes into account the projected shapes of the subducted parts of the Nazca Ridge and the Inca Plateau. Accordingly, the geometry of these ridges prior to their subduction were deduced from the shape of their conjugate features on the Pacific plate considering that the two pairs of topographic anomalies formed simultaneously during symmetric sea-floor spreading at the East Pacific Rise. Thus, the shape and the length of the original Inca Plateau in the reconstruction is the mirror image of the present-day Marquesas Plateau.

In this reconstruction the Inca Plateau would have reached the south-western area of the present Marañón Basin during the Pliocene (around 4Ma). The timing and the areal extension of the uplift described in this study are consistent with this reconstruction, and so is the decrease in basal HF.

We documented in this work how the subduction of an aseismic ridge could trigger a flattening of the subducting slab and a retreat of the asthenospheric wedge below the overriding plate. T placing the observations from the Marañón Basin in this global framework, we could explain

Geologica Acta, 12(4), 287-306 (2014)
DOI: 10.1344/GeologicaActa2014.12.4.2

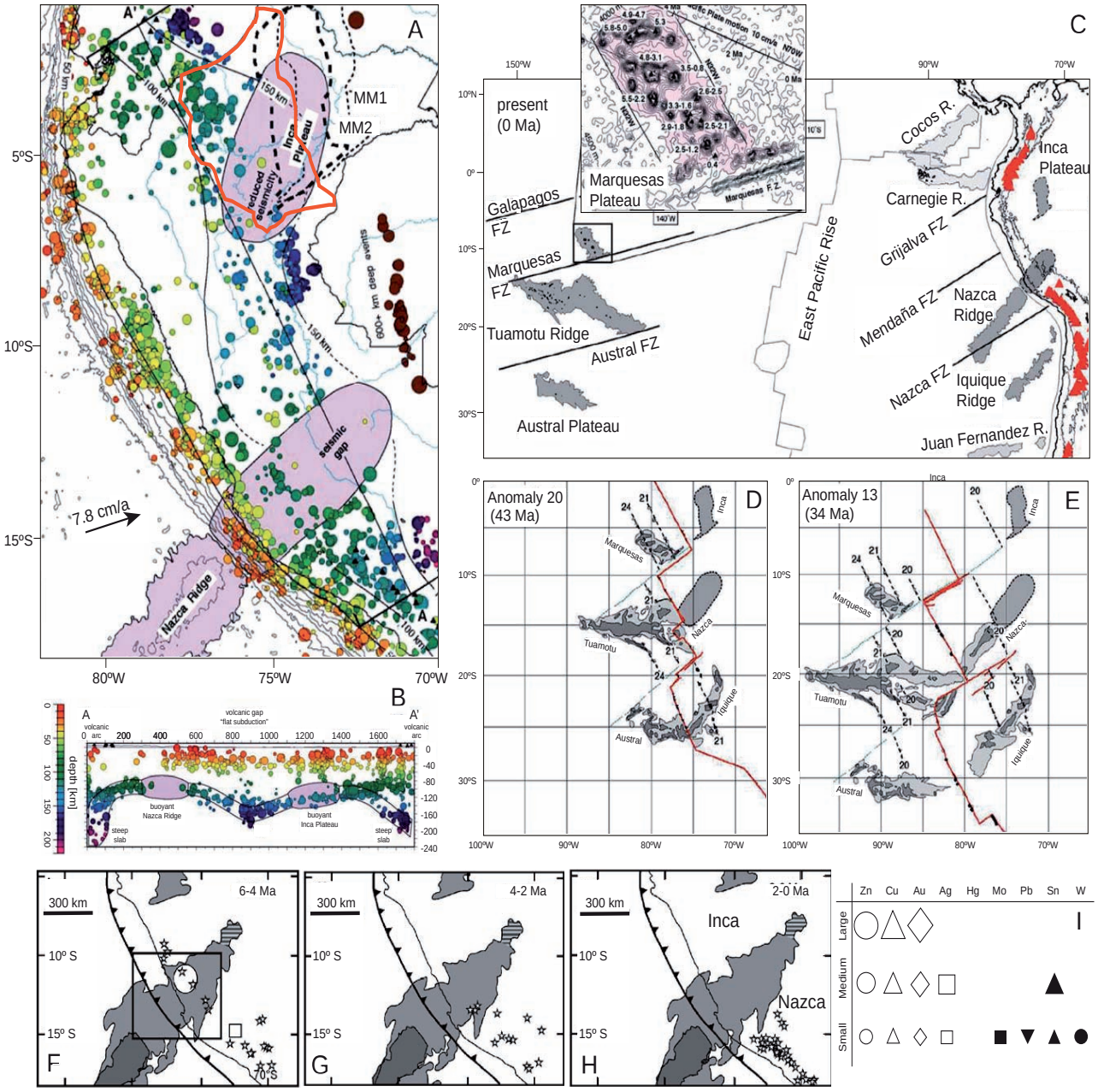

FIGURE 9. Montage illustrating the evidences for the subduction of the lost Inca oceanic plateau underneath the SW of the Marañon basin. A) Seismicity (1964-1995) at more than 200km from the trench omitting shallow events (<70km) (Gutscher et al.,1999b). The Marañón basin is outlined in red. Notice how the present position of the Inca Plateau (MM2 doted outline) and the related area of reduced seismicity (grey shaded) coincides with the anomaly of the present day heat flow map of figure 7. Arrow indicates the relative convergence of the Nazca plate with velocity. Depth contours to Wadati-Benioff zone are in kilometers. Location of Marquesas mirror image (MM1) from direct kinematic reconstruction (in the same figure) and after an 80km correction (MM2) for dip of Nazca Plate to 150km depth; B) Seismological section A-A' beneath the Andes (location on A, Gutscher et al., 1999b) showing how steep slab segments at the N and S end with active arc volcanism (black triangles). The 1500km long flat slab portion is supported by the Nazca ridge and Inca Plateau buoyant bodies with intervening sag. C) Tectonic setting of oceanic plateaus and the Andean margin with active volcanoes (red triangles), currently active spreading center (East Pacific Rise) and major fracture zones (FZ) (Gutscher et al., 1999b). Subducted portion of Nazca Ridge and the position of the Marquesas mirror image (Inca Plateau) are shown dashed. Inset is a bathymetric map of Marquesas Archipelago with age dates for recent volcanoes; D) and E) are reconstructions of Farallon-Pacific spreading center at Chron 20 (43Ma) and Chron 13 (34Ma) respectively. F,G,H: Reconstruction of the subduction history of the Nazca Ridge and the Inca Plateau between 6 and 0Ma from Rosenbaum et al. (2005). Each reconstruction corresponds to the average age of the annotated time interval and shows location of ore deposits and volcanic centres that were active during that interval. Arc volcanism is indicated by stars. Ore deposits are shown by geometric symbols indicating their nature and relative size (legend in image I). The location of the present day non-subducted part of the Nazca Ridge is indicated by dark grey. The subducted portion and the Inca Plateau are in light grey and the striped area indicates the mirror image of the northwestern tip of the Tuamotu Plateau.

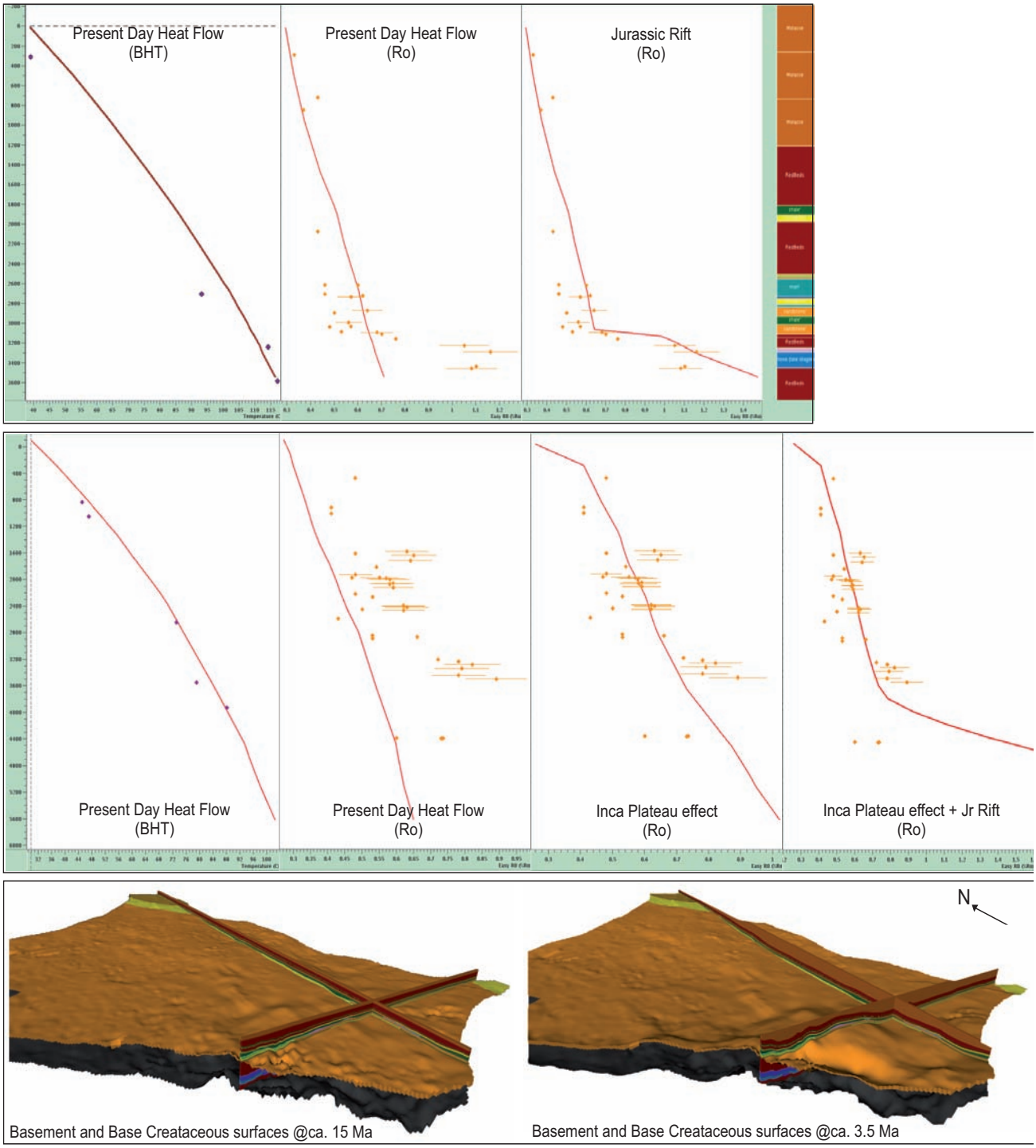

FIGURE 10. Work flow for basin model thermal history definition illustrated through calibration at a well located in the North of the Marañon basin (upper row diagrams) and at a well located in the SW (lower row diagrams). Red curves are calculated values, violet dots are corrected measured temperatures and yellow dots are measured vitrinite reflectance with error bars. The uplift and related erosion associated to the Inca Plateau effect is illustrated with 3D structural views of the model at ca. 15 and 3.5 Ma. Step 1) definition of a present day basal heat flow (HF) map that allows calibrating the calculated temperature at well location with measured borehole and production corrected temperatures; Step 2) present day HF applied through time: the model calibrates with maturity data (Ro) of the Cretaceous-III mega-sequence in the northern part of the basin but the actual thermal regime is too low for the south-western wells; Step 3) increased basal HF in the SW prior to 4 Ma, estimated age of the Inca Plateau arrival in this area of the basin, and related uplift and erosion between 4 and 3,5 Ma; Step 4) rifting (high) HF type applied prior to the Base Cretaceous Unconformity allowing to match the maturity indicators from the Jurassic sequence.

Geologica Acta, 12(4), 287-306 (2014)
DOI: 10.1344/GeologicaActa2014.12.4.2

the recent uplift and erosion observed in the south-western part of the basin by an increase in deformation resulting from a stronger coupling of both plates following the subduction of the Inca Plateau. Thermically, the forced retreat of the asthenospheric wedge following the flattening of the subducting slab could have caused a retreat of the isotherms and be responsible for a decrease of the basal heat flow entering this area of the basin and the subsequent colder thermal regime.

CONCLUSION

The postulated Inca Plateau subduction effects on thermics and deformation provide a realistic scenario for the recent evolution of the Marañón Basin. In terms of petroleum system modelling the possibility to relate conclusions on the thermal regime derived from measured data, such as well temperatures and maturity indicators, with global dynamics through time allowed us to build a more reliable scenario for thermal history, that is one of the major controlling factor, if not the main one, for hydrocarbons generation.

To summarize, the following workflow was used to define the thermal regime at present and through time (Fig. 10): i) definition of a present day basal heat flow map that allows calibrating the calculated actual temperatures at well location with measured borehole and production temperatures; ii) present day HF applied through time: the model calibrates with maturity data of the Cretaceous-III megasequence in the northern part of the basin, but the actual thermal regime is too low for the south-western wells; iii) increased basal HF in the south-west prior to 4Ma, age of the Inca Plateau arrival in this area of the basin, and related uplift and erosion between 4 and 3,5Ma; iv) rifting (high) HF type applied prior to the base Cretaceous unconformity allowing to match the maturity indicators of the Jurassic sequence.

This study documents the consequences of the subduction of an oceanic plate topographic anomaly on the thermal regime of the foreland Marañón Basin of Perú during Neogene. Maturity indicators showed an anomaly that spatially coincides with the subduction trace of a lost ridge, the Inca Plateau. Other features like differential uplift and erosion can be related to the same event in this area. In addition, it can be inferred that the uplift may have locally modified the migration pathways and fetch areas in both source and reservoir layers.

The effects of ridge subduction on the deformation and volcanism of the Andean forearc and arc regions have been extensively described. Their influence on the present day foreland topography is testified by the existence of giant alluvial fans and displaced terraces. Their effect on magmatism and ore deposits formation has also been demonstrated. The example of the Marañón Basin shows that their influence on thermal regime, deformation, erosion and ultimately on petroleum systems, must also be taken into account in the search for hydrocarbons in subduction related basins.

ACKNOWLEDGMENTS

The authors want to acknowledge Professor Dr. V.A. Ramos for his thoughtful review, as well as N. Chigne that contributed to the improvement of the manuscript sharing its deep experience of oil exploration in Perú. They also are thankfull to ALAGO for allowing them to present in the 2012 Congress of Santa Marta (Colombia). Data and conclusions from Perú are part of a Repsol internal project on the Petroleum Potential of the Marañón Basin. The authors thank the direction of the Geology Department at Repsol Exploration S.A. in Madrid and Repsol Perú for authorizing the publication of this information. They are also grateful to O. San Juan Palomares for her help in the illustration drawings.

REFERENCES

Barazangi, M., Isacks, B.L., 1976. Spatial distribution of earthquakes and subduction of the Nazca plate beneath South America. Geology, 4, 686-692.

Baudino, R., 1995. Evolution des Andes d`Equateur au Neogene: les enseignements de l'étude des bassins intramontagneux, Doctoral Thesis. France, Pau University, 431pp.

Baudino, R., Hermoza, W., 2011. Effect of oceanic ridge subduction on Andean foreland basins: implications for thermal regime. Extended Abstracts of the 7th INGEPET, Lima, Perú, 7-11th November 2011.

Bés de Berc, S., Baby, P., Soula, J.-C., Rasero, J., Souris, M., Christophoul, F., Vega J., 2004. La superficie mera-upano: marcador geomorfológico de la incisión fluviatil y del levantamiento tectónico de la zona subandina ecuatoriana. In: Baby, P., Barragan, R., Rivadeneira, M., (eds.). La cuenca Oriente: geologia y petróleo, Travaux de l'Institut Français d'Études Andines, 144, 153-168.

Bevis, M., 1986. The curvature of Wadati-Benioff zones and the torsional rigidity of subducting plates. Nature, 323, 52-53.

Bird, P., 1988. Formation of the Rocky Mountains, western United States: a continuum computer model. Science, 239, 1601-1507.

Cahill, T., Isacks, B.L., 1992. Seismicity and shape of the subducted Nazca Plate. Journal of Geophysical Research, 97, 17503-17529.

Chung, W.Y., Kanamori, H., 1978. A mechanical model for plate deformation associated with aseismic ridge subduction in the New Hebrides Arc. Tectonophysics, 50, 29-40.

Clift, P.D., Pecher, I., Kukowski, N., Hampel, A., 2003. Tectonic erosion of the Peruvian forearc, Lima Basin, by subduction and Nazca Ridge collision. Tectonics, 22, 1023-1042.

Cloos, M., 1993. Lithospheric buoyancy and collisional orogenesis: subduction of oceanic plateaus, continental margins, island arcs, spreading ridges, and seamounts. Geological Society of America Bulletin, 105, 715-737.

Cox, S.F., Braun, J., Knackstedt, M.A., 2001. Principles of structural control on permeability and fluid flow in hydrothermal systems. Reviews in Economic Geology, 14, 1-24.

Cross, T.A., Pilger Jr., R.H., 1982. Controls of subduction geometry, location of magmatic arcs, and tectonics of arc and back-arc regions. Geological Society of America Bulletin, 93, 545-562.

Dickinson, W.R., Snyder, W.S., 1979. Geometry of subducted slabs related to the San Andreas transform. Journal of Geology, 87, 609-627.

Domínguez, S., Malavielle, J., Lallemand, S.E., 2000. Deformation of accretionary wedges in response to seamount subduction: insights from sandbox experiments. Tectonics, 19, 182-196.

English, J., Johnston, S.T., Wang, K., 2003. Thermal modeling of the Laramide orogeny: Testing the flat slab subduction hypothesis. Earth and Planetary Science Letters, 214, 619-632.

Espurt, N., Baby, P., Brusset, S., Roddaz, M., Hermoza, W., Regard, V., Antoine, P.-O., Salas-Gismondi, R., Bolaños, R., 2007. How does the Nazca Ridge subduction influence the modern Amazonian foreland basin? Geology, 35, 515-518.

Fernández, J., Martinez, E., Calderon, Y., Galdos, C., 2002. The Pucara Petroleum System and the pre-Cretaceous sabkha regional seal, a new hydrocarbon play in the Peruvian fold thrust belt. Proceedings from the 2002 Ingepet.

Gephart, J.W., 1994. Topography and subduction geometry in the central Andes: clues to the mechanics of a monocollisional orogen. Journal of Geophysical Research, 99, 279-288.

Groome, W.G., Thorkelson, D.J., 2009. The three-dimensional thermo-mechanical signature of ridge subduction and slab window migration. Tectonophysics, 464, 70-83.

Gutscher, M.A., 2002. Andean subduction styles and their effect on thermal structure and interplate coupling. Journal of South American Earth Sciences, 15, 3-10.

Gutscher, M.A., Malavieille J., Lallemand S., Collot J.-Y., 1999a. Tectonic segmentation of the North Andean margin: Impact of the Carnegie Ridge collision. Earth and Planetary Science Letters, 168, 255-270.

Gutscher, M.A., Olivet J.L., Aslanian D., Eissen J.P., Maury R., 1999b. The lost Inca Plateau: cause of flat subduction beneath Perú? Earth and Planetary Science Letters, 171, 335-341.

Gutscher, M.A., Spakman, W., Bijwaard, H., Engdahl, E.R., 2000a. Geodynamics of flat subduction: seismicity and tomographic constraints from the Andean margin. Tectonics, 19, 814-833.

Gutscher, M.-A., Maury, R., Eissen, J.-P., Bourdon, E., 2000b. Can slab melting be caused by flat subduction? Geology, 28, 535-538.

Hampel, A., 2002. The migration history of the Nazca Ridge along the Peruvian active margin: a re-evaluation. Earth and Planetary Science Letters, 203, 665-679.

Hampel, A., Kukowski, N., Bialas, J., Huebscher, C., Heinbockel, R., 2004. Ridge subduction at an erosive margin: the collision zone of the Nazca Ridge in southern Perú. Journal of Geophysical Research, 109, 1-19.

Henry, S.G., Pollack H.N., 1988. Terrestrial heat flow above the Andean subduction zone in Bolivia and Perú. Journal of Geophysical Research, 93, 153-162.

Hildreth, W., Moorbath, S., 1988. Crustal contributions to arc magmatism in the Andes of Central Chile. Contributions to Mineral Petrology, 98, 455-489.

Irifune, T., Ringwood, A.E., 1993. Phase transformations in subducted oceanic crust and buoyancy relations at depths of 600–800km in the mantle. Earth and Planetary Science Letters, 117, 101-110.

Isacks, B.L., Barazangi, M., 1977. Geometry ofBenioff zones: Lateral segmentationand downwards bending of the subducted lithosphere. In: Pitman, W., Talwani, M. (eds.). Island Arcs, Deep sea trenches and Back Arc Basins, American Geophysical Union, Ewing Series, 1, 99-114.

Jischke, M.C., 1975. On the dynamics of descending lithospheric plates and slip zones. Journal of Geophysical Research, 80, 4809-4813.

Jordan, T.E., Isacks, B.L., Allmendinger, R.W., Brewer, J.A., Ramos, V.A., Ando, C.J., 1983a. Andean tectonics related to geometry of subducted Nazca plate. Geological Society of America Bulletin, 94, 341-361.

Jordan, T.E., Isacks, B.L., Ramos, V.A., Allmendinger, R.W., 1983b. Mountain building in the Central Andes. Episodes, 97, 20-26

Kay, S.M., Mpodozis, C., Ramos, V.A., Munizaga, F., 1991. Magma source variations for mid-late Tertiary magmatic rocks associated with a shallowing subduction zone and thickening crust in the central Andes (28-33ºS). In: Harmon, R.S., Rapela, C.W. (eds.). Andean Magmatism and its Tectonic Setting. Geological Society of America, Special paper, 26, 113-137.

Kay, S.M., Abbruzzi, J.M., 1996. Magmatic evidence for Neogene lithospheric evolution of the central Andean "flat-slab" between 30°S and 32°S. Tectonophysics, 259, 15-28.

Kellogg, J., Vega, V., 1995. Tectonic development of Panama, Costa Rica, and the Colombian Andes: constraints from global positioning system geodetic studies and gravity. In: Mann, P. (ed.), Geologic and Tectonic Development of the Caribbean plate Boundary in Southern Central America. Geological Society of America Bulletin, Special Paper, 295, 75-89.

Kirby, S., Engdahl, R., Denlinger, R., 1996a. Intermediate-depth intraslab earthquakes and arc volcanism as physical expressions of crustal and uppermost mantle metamorphism in subducting slabs. Subduction: Top to Bottom. American Geophysical Union, 96, 195-214.

Lonsdale, P., 1978. Ecuadorian subduction system. American Association of Petroleum Geologists Bulletin, 62, 2454-2477.

Marocco, R., Lavenu, A., Baudino, R., 1995. Intermontane Late Paleogene-Neogene Basins of the Andes of Ecuador and Perú: Sedimentologic and Tectonic Characteristics. In: Suarez Soruco, R., Tankard, A.J., Welsink, H.J. (eds.), Petroleum Basins of South America. American Association of Petroleum Geologists, Memoir 62, 597-614.

McGeary, S., Nur, A., Ben-Avraham, Z., 1985. Spatial gaps in arc volcanism: the effect of collision or subduction of oceanic plateaus. Tectonophysics, 119, 195-221.

McNulty, B., Farber, D., Patriat, P., Torres, V., Sempere, T., 2003. Paleomagnetic tracking of mountain building in the Peruvian Andes since 10Ma. Tectonics, 22, 1048-1062.

Murphy, J.B., 2007. Igneous Rock Associations 7: Arc Magmatism I: Relationship Between Subduction and Magma Genesis. Geoscience Canada, 33(4).

Nur, A., Ben-Avraham, Z., 1981. Volcanic gaps and the consumption of aseismic ridges in South America, In: Dasch, E.J., Dymond, J., Hussong, D.M., Kulm, L.D., Roderick, R. (eds.), Nazca Plate: Crustal Formation and Andean Convergence. Geological Society of America, Memoir 154, 729-740.

Pardo, M., Comte, D., Monfret, T., 2002. Seismotectonic and stress distribution in the central Chile distribution zone. Journal of South American Earth Sciences, 15, 11-22.

Pilger, R.H., 1981. Plate reconstructions, aseismic ridges, and low angle subduction beneath the Andes. Geological Society of America Bulletin, 92, 448-456.

Ramos, V.A., 1999. Plate tectonic setting of the Andean Cordillera. Episodes, 22(3), 183-190.

Ramos, V.A., Munizaga, F., Kay, S.M., 1991. El magmatismo cenozoico a los 33ºS de latitud: Geocronología y relaciones tectónicas. VI Congreso Geológico Chileno (Viña del Mar), Actas 1, 892-896.

Ramos, V.A., Cristallini, E.O., Perez, D.J., 2002. The Pampean Flat Slab of the Central Andes. Journal of South American Earth Sciences, 15, 59-78.

Ramos, V.A., Zapata, T., Cristallini, E., Introcaso, A., 2004. The Andean thrust system— Latitudinal variations in structural styles and orogenic shortening. In: Mc Clay, K.R. (ed.), Thrust tectonics and hydrocarbon systems. American Association of Petroleum Geologists, Memoir 82, 30-50.

Ramos, V.A., Folguera, A., 2009. Andean flat slab subduction through time. In: Murphy, B. (ed.), Ancient Orogens and Modern Analogues. London , The Geological Society, Special Publication, 327, 31-54.

Ranero, C.R., von Huene, R., 2000. Subduction erosion along the Middle America convergent margin. Nature, 404, 748-752.

Richards, J.P., 2003. Tectono-magmatic precursors for porphyry Cu-(Mo–Au) deposit formation. Economic Geology, 98, 1515-1533.

Rosas, S., Fontbote, L., Tankard, A., 2007. Tectonic evolution and paleogeography of the Mesozoic Pucara Basin, central Perú. Journal of South American Earth Sciences, 24, 1-24.

Rosenbaum, G., Giles, D., Saxon, M., Betts, P.G., Weinberg, R.F., Duboz, C., 2005. Subduction of the Nazca Ridge and the Inca Plateau: Insights into the formation of ore deposits in Perú. Earth and Planetary Science Letters, 239, 18-32.

Sacks, I.S., 1983. The subduction of young lithosphere. Journal of Geophysical Research, 88 (B4), 3355-3366.

Schneider, J.F., Sacks, I.S., 1987. Stress in the contorted Nazca Plate beneath Southern Perú from local earthquakes. Journal of Geophysical Research, 92, 13887-13902.

Smalley, R., Pujol, J., Regnier, M., Chiu, J.-M., Chatelain, J.L., Isacks, B.L., Araujo, M., Puebla, N., 1993. Basement seismicity beneath the Andean Precordillera thin skinned
thrust belt and implications for crustal and lithospheric behavior. Tectonics, 12, 63-76.

Smith, W.H.F., Sandwell, D.T., 1997. Global seafloor topography from satellite altimetry and ship depth soundings. Science, 277, 1957-1962.

Stern, C.R., 2004. Active Andean volcanism: its geologic and tectonic setting. Revista Geológica de Chile, 31(2), 161-206.

Stevenson, D.J., Turner, S.J., 1977. Angle of subduction. Nature, 270, 334-336.

Suarez, G., Molnar, P., Burchfiel, B.C., 1983. Seismicity, fault plane solutions, depth of faulting, and active tectonics of the Andes of Perú, Ecuador and S. Colombia. Journal of Geophysical Research, 88, 10403-10428.

Tamura, Y., Tatsumi, Y., Zhao, D.P., Kido, Y, Shukuno, H., 2002. Hot fingers in the mantle wedge: new insights into magma génesis in subduction zones. Earth and Planetary Science Letters, 197, 105-116.

Thorpe, R.S., 1984. The tectonic setting of active Andean volcanism. In: Barreiro, B.A., Harmon, R.S., (eds). Andean magmatism: Chemical and Isotopic Constraints. Nantwich, U.K., Shiva Geological Series, Shiva Publications, 4-8.

Tovish, A., Schubert, G., Luyendyk, B.P., 1978. Mantle flow pressure and the angle of subduction: non-Newtonian corner flows. Journal of Geophysical Research, 83(B12), 5892-5898.

Van Hunen, J., van der Berg, A.P., Vlaar, N.J., 2002. On the role of subducting oceanic plateaus in the development of shallow flat subduction. Tectonophysics, 352, 317-333.

Vlaar, N.J., 1983. Thermal anomalies and magmatism due to lithospheric doubling and shifting. Earth and Planetary Science Letters, 65, 322-330.

Van Keken, P.E., Kiefer, B., Peacock, S.M., 2002. High-resolution models of subduction zones: Implications for mineral dehydration reactions and the transport of water into the deep mantle. Geochemistry, Geophysics, Geosystems, 3(10), 1056.

Von Huene, R., Corvalan, J., Flueh, E.R., Hinz, K., Korstgard, J., Ranero, C.R., Weinrebe, W., the Condor Scientists, 1997. Tectonic control on the subducting Juan Fernandez Ridge on the Andean margin near Valparaiso, Chile. Tectonics, 16, 474-488.

Von Huene, R., Lallemand S., 1990. Tectonic erosion along the Japan and Perú convergent margins. Geological Society of America Bulletin, 102, 704-720.

Von Huene, R., Pecher, I.A., Gutscher, M.-A., 1996. Development of the accretionary prism along Perú and material flux after subduction of Nazca Ridge. Tectonics, 15, 19-33.

Von Huene, R., Suess E., 1988. Leg 112 Shipboard Scientific Party, Ocean Drilling Program Leg 112, Perú continental margin: Part 1: Tectonic history. Geology, 16, 934-938.

Waples, D., 2002. Oil Families in the Marañón Basin. Internal Report of Apex Petroleum Inc., a subsidiary of RepsolYPF.

Manuscript received March 2014;
revision accepted October 2014;
published Online November 2014.

Geologica Acta, 12(4), 287-306 (2014)
DOI: 10.1344/GeologicaActa2014.12.4.2